Desalination and Water Treatment
www.deswater.com

doi: 10.5004/dwt.2022.28518

261 (2022) 278–288
June

Facile synthesis of silica nanoparticles with cationic surfactant and investigation of equilibrium, kinetics and thermodynamics of Reactive Yellow 42 dye removal from aqueous solutions

Ali Naghizadeh[a,*], Nourahmad Nourafrouz[b], Elham Derakhshani[a], Majid Asri[c,*], Marzieh Esmati[d]

[a]*Medical Toxicology and Drug Abuse Research Center (MTDRC), Birjand University of Medical Sciences, P.O. Box: 9717853577, Birjand, Iran, Tel. +985632381665; Fax: +985632395346; email: al.naghizadeh@yahoo.com (A. Naghizadeh)*
[b]*Department of Environmental Health Engineering, Student Research Committee, Faculty of Health, Birjand University of Medical Sciences, Birjand, Iran, email: noorafrozn1@mums.ac.ir (N. Nourafrouz)*
[c]*Department of Environmental Health Engineering, Faculty of Medicine Sciences, Islamic Azad University, Birjand Branch, Birjand, Iran, email: majid.asri@yahoo.com (M. Asri)*
[d]*Medical Toxicology and Drug Abuse Research Center (MTDRC), Birjand University of Medical Sciences, Birjand, Iran, email: m.esmaty1993@yahoo.com (M. Esmati)*

Received 6 November 2021; Accepted 19 April 2022

ABSTRACT

Reactive Yellow 42 (RY 42) dye is a synthetic azo dye which is very important and also is widely used industries. Therefore, the aim of this study was to synthesize silica nanoparticles and to investigate the equilibrium, kinetics and thermodynamics of the removal of RY 42 dye by these nanoparticles from aqueous solutions. This study was performed on a laboratory scale. First, silica nanoparticles were fabricated with cationic surfactant and then field-emission scanning electron microscopy, X-ray diffraction and Fourier-transform infrared spectroscopy techniques were used to evaluate its properties. Also, the effect of various parameters such as pH (3–11), nanoparticle dose (0.1–0.6 g/L), contact times of 10–120 min and initial dye concentrations (50–10 mg/L) in adsorption reaction were investigated. Finally, the kinetics, isotherms and thermodynamics of the reaction were determined. According to the results of this study, as the RY 42 dye concentration increased, the removal rate decreased, resulting in lower efficiencies. Also, the highest removal percentage of RY 42 dye at pH = 3, initial concentration of 10 mg/L, adsorbent dosage of 0.1 g/L and contact time of 120 min was occurred and was equal to 94.1%. The isotherm and kinetics of the adsorption reaction followed the Langmuir model and the pseudo-second-order model, respectively. Free energy changes of Gibbs (ΔG), enthalpy changes (ΔH) and entropy changes (ΔS) were obtained in this study. Since (ΔG) is negative, (ΔH) is positive, and (ΔS) is positive, the process is endothermic and spontaneous. Therefore, the adsorption process by silica nanoparticles is a suitable option for removal of RY 42 dye from aqueous and wastewater solutions and can be used as an efficient and suitable adsorbent.

Keywords: Synthesis; Silica nanoparticles; Kinetics; Thermodynamics; Isotherms; Reactive dyes

* Corresponding authors.

1. Introduction

Today, environmental pollution is one of the global problems and dilemmas [1]. One of the most important environmental pollutants is industrial wastewater, which due to the diversity and difference in the nature of chemicals used in industrial processes, makes it difficult and complex to treat [2]. Among these various pollutants, dyes are among the mineral and organic compounds that are produced about one million tons per year in various parts of human daily life in the world [3–6]. Colored effluents are produced in many industries such as textiles, paper, printing, leather, tanning, inks, cosmetics, etc. and therefore enter the environment.

Textile dyes are the largest group of water soluble synthetic dyes that have the greatest variety in terms of type and structure [7]. Dyes are divided into azo, anthraquinone, xanthine, acridine, flavin, cyanine, ethane, etc. based on their chemical structure, and in terms of application, they are reactive, acidic, direct, bent, dispersed and etc. [8]. Dyes are detectable in very small amounts, even around 1 mg/L, and affect aquatic life as well as general health [9]. Studies have shown that the dyes used in the textile industry are carcinogenic and mutagenic and also cause allergies, dermatitis and skin irritation [10–15]. Also, the entry of colored effluents into the receiving waters prevents the complete passage of light into the water and consequently reduces the action of photosynthesis and thus reduces the dissolved oxygen and the phenomenon of eutrophication [16]. The dye, on the other hand, binds to metal ions to form compounds that are toxic to fish and other microorganisms in the water. Therefore, environmental researchers have always sought to eliminate these hazardous compounds [17].

Reactive Yellow 42 (RY 42) is also a synthetic azo dye that is very important and widely used. More than 27.2% of the textile industry uses this dye. Most of these colors cause many problems in humans, including dermatitis and itchy skin. They also accelerate cancer and mutagenicity in humans [18].

There are various methods for decolorizing the textile industry effluent that can be coagulation and flocculation, chemical oxidation, biological treatment, electrochemical technique, ion exchange, adsorption and combined processes including ozonation and coagulation [19–21]. Each of these methods has advantages and disadvantages. Conventional wastewater treatment processes such as coagulation and flocculation, chemical precipitation are not effective methods for their removal due to the formation of strong and biodegradable complexes in most dyes of the textile industry. These methods also produce a lot of sludge, which causes many environmental problems. Advanced treatment processes are often expensive and also require specialized labor to operate. Biological treatment processes are not possible due to the synthetic and aromatic structure of colored effluents [22]. Among the other methods, the adsorption process, due to its high potential for the removal of micro molecular materials, including dyes and organic matter, seems to be one of the best solutions for the treatment of colored effluents. Many advantages of the adsorption process over other conventional treatment processes include low surface area used, low sensitivity to flow fluctuations, no effect of toxic chemicals in the process, high flexibility in process design and implementation, and very high removal of organic matter [23]. In the same field, the adsorbents used to remove the dye from the effluent can be chitin and chitosan [24,25], single-walled carbon nanotubes [26,27], pumice mineral adsorbent [28], bone ash [29], barberry stem powder [30] activated carbon prepared from walnut wood [31] mentioned. Activated carbon is one of the most widely used adsorbents, but due to the high cost of production, those studies are being revived to obtain alternative adsorbents with higher adsorption capacity and lower cost. In this regard, the use of nanotechnology methods has received much attention today. Nanoparticles can be used to treat contaminants due to their small size, high cross-section, crystallinity and therefore high reactivity [32–35].

Nanotechnology is a rapidly growing field and now it has had far-reaching effects in various areas of human life, including applications in the environment, wire, industry, agriculture, and medicine. Nanoparticles have unique chemical, physical and optical properties due to their nanoscale size and high surface-to-volume ratio [36]. Meanwhile, SiO_2 is composed of two elements, silicon and oxygen, and is structurally similar to the structure of a water molecule. SiO_2 is a major component of soil that is used as a base material for bacterial growth due to its non-toxicity. Studies show that SiO_2 nanoparticles can be used as adsorbents to remove natural contaminants and metal ions as well as a variety of dyes [37]. The aim of this study was to synthesis of silica nanoparticle as well as investigate the equilibrium, kinetics and thermodynamics of the removal of RY 42 dye by silica nanoparticles from aqueous solutions.

2. Materials and methods

In this laboratory study, synthesized silica nanoparticles, RY 42 dye (Alvan Sabet Company) were used. The devices used include the British PG Spectrophotometer Model UV/Vis Spectrometer T80+, Fourier-transform infrared spectroscopy device (FTIR) using the model device (AVATAR 370) with spectrometer spectrum in the range of 400–4,000 cm^{-1} and vegetative electron microscope FESEM model (SIGMA VP–, Zeiss, Germany) as well as X-ray diffraction (XRD) model (Pert PRO X made by Panalytical Company).

2.1. Synthesis and preparation of silica nanoparticles

For synthesis of silica nanoparticles, the cationic surfactant cetyltrimethylammonium bromide (CTMABr) was used as template and tetraethyl orthosilicate (TEOS) was used as the silica source. The polymerization process of the silica source was performed in basic and acidic media using HCl as catalysts.

First, 1.1 g of CTMABr surfactant was dissolved in 45 mL of deionized water with complete vigorous stirring. Then 30 mL of hydrochloric acid was added and given 10 min to obtain a milky and uniform solution. Finally, 0.003 mol TEOS is added dropwise to the solution and then allowed to produce a milky jelly solution the resulting solution is placed in a water bath at a temperature of 70°C. After 1 h, it is dried at 80°C and then calcined for 6 h at 540°C [38].

2.2. Adsorption experiment

All adsorption experiments were performed on batch condition and laboratory scale. The effect of various parameters such as initial pH, contact time, adsorbent dose and initial concentration of RY 42 dye was examined. For this purpose, stock solution (1,000 mg/L) of RY 42 dye was prepared by dissolving certain amounts of RY 42 dye in deionized water. Then a certain amount of RY 42 dye solution was prepared with a certain pH and in Erlenmeyer it was stirred with a certain contact time by shaker. The residual amount of RY 42 dye was read using a UV/Vis spectrophotometer machine at 430 nm.

In all stages of the experiments, the efficiency and adsorption capacity were calculated using Eqs. (1) and (2) respectively. To calculate the removal efficiency Eq. (1) was used, where R is the removal efficiency (%), C_t is the residual concentration of the RY 42 dye at time t (mg/L), and C_0 is the initial concentration of RY 42 dye (mg/L).

$$\%R = \frac{C_0 - C_t}{C_0} \times 100 \tag{1}$$

Eq. (2) was also used to calculate the equilibrium adsorption capacity.

$$q_e = \frac{\left(C_0 - C_e\right) \times V}{M} \tag{2}$$

where q_e is equilibrium capacity (mg/g), C_0 and C_e are the initial concentration and residual concentration of RY 42 dye at time "t" (mg/L), V is solution volume (L) and M is adsorbent dose (g). [39]

2.3. Adsorption isotherms

In this study, the Langmuir and Freundlich adsorption isotherm model in adsorption of RY 42 dye were used. The Langmuir isotherm is based on the monolayer and homogenous adsorption of the adsorbate material with the same energy on all surfaces on the adsorbent.

Freundlich isotherm is based on monolayer and heterogeneous adsorption of adsorbent on adsorbent. The Freundlich isotherm is based on the monolayer and heterogeneous adsorption of adsorbate material on the adsorbent. In fact, in the Freundlich model, it is assumed that the adsorption is monolayer and non-uniform [40]. The following equation represents the Freundlich isotherm model.

$$q_e = K_f C_e^{1/n} \tag{3}$$

where q_e is equilibrium concentration of solid contaminant (mg/L), K_f is Freundlich constant and C_e is equilibrium concentration (mg/L).

In the Langmuir adsorption isotherm, adsorption is monolayer and the adsorption regions on the surface of the adsorbent are uniform and also all have the same adsorption power. Adsorption joints and bonds are also reversible. The following equation represents the Langmuir isotherm model.

$$\frac{C_e}{q_e} = \frac{1}{q_{\max} K_L} + \frac{C_e}{q_{\max}} \tag{4}$$

where $q_{\max}$ is the maximum adsorption rate (mg/g), K_L is the Langmuir adsorption equilibrium constant, C_e is the equilibrium concentration (mg/L) and q_e is the equilibrium concentration of the solid phase contaminant (mg/L).

2.4. Adsorption kinetics

Two common models of kinetic (pseudo-first-order and pseudo-second-order kinetics) were used for studying the kinetic of adsorption. The correlation coefficient (R^2) has been considered as a criterion for agreement between the experimental data and two suggested models [39].

The pseudo-first-order kinetic or equation is as follows:

$$\log\left(q_e - q_t\right) = \log q_e - \frac{k_1}{2.303} t \tag{5}$$

where q_e: the rate of the adsorbed material on the adsorbent in the time t according to mg/g; q_t: the rate of the adsorbed material on the adsorbent in the equilibrium time according to mg/g; K_1: the adsorption rate constant pseudo-first-order kinetic (L/min).

The chart of log ($q_e - q_t$) against t is used for determining the k constant and q_e.

The pseudo-second-order kinetic equation is as follows:

$$\frac{t}{q_t} = \frac{1}{K_2 q_e^2} + \frac{1}{q_e} \tag{6}$$

where K_2 is a pseudo-second-order kinetic adsorption rate constant (g/(mg min)). The graph of t/q_t vs. t is used to obtain velocity parameters. The values of K_2 and q_e are obtained by calculating the width from the origin and the slope.

2.5. Determination of the optimal temperature

Then, by keeping all the optimal parameters obtained from the previous steps (pH, contact time, adsorbent dose and dye concentration), the experiment was performed at temperatures of 15°C, 25°C, 35°C and 50°C. In the next step, using adsorption thermodynamic constants including change of Gibbs free energy ($\Delta G°$), entropy change ($\Delta S°$) and enthalpy change ($\Delta H°$) were investigated. In this step, Eqs. (7) and (8) were used to determine the thermodynamic constants.

$$\Delta G = -RT \ln K \tag{7}$$

$$\ln K = \frac{\Delta S}{R} - \frac{\Delta H}{RT} \tag{8}$$

where K: thermodynamic equilibrium constant, C_S: dye adsorption concentration in solution by adsorbent (mg/L), C_e: dye residue concentration in equilibrium solution (mg/L), R: global gas constant (314.8 J/mol K), T is the absolute temperature in Kelvin [40].

3. Results and discussion

3.1. Determination of silica nanoparticles properties

3.1.1. FTIR spectra

FTIR analysis was used to determine the functional groups of silica nanoparticles. Fig. 1 represents the desired spectrum.

According to Fig. 1, peak in 1,076.7 cm^{-1} related to Si–O–Si asymmetric band, peak in 805.54 cm^{-1} is related to Si–O–Si symmetric bands, and 458.23 cm^{-1} Bending is related to vibrations Si–O–Si, peak in 1629.85 is related to the bending vibrations of the hydroxyl group. A wide band absorbed in the region 3,100–3,700 cm^{-1} is related to the reaction of Si–OH with water molecules.

3.1.2. Scanning electron microscopy image

Scanning electron microscopy analysis was used to prove the nanoparticle scale, porosity size and distribution and to investigate the roughness and unevenness of the adsorbent surface (Fig. 2).

According to the images, it is clear that all the particles are in a spherical shape, which confirms how the cylinders of surfactants are arranged.

3.1.3. XRD analysis

Fig. 3 shows the XRD pattern of SiO_2 nanoparticles. In XRD experiment, X-ray diffraction was used to determine the amount of crystalline and non-crystalline phase of the adsorbent. The peak at 2θ = 10°–25° is related to the presence of amorphous silica.

3.2. Effect of different parameters on the adsorption of RY 42 dye by silica nanoparticles

3.2.1. Determination of pH_{zpc}

To determine pH_{zpc} (point of zero charge), distilled water solutions were prepared with pH between 2–12 using HCl and NaOH (1 and 0.1 N). Then, 25 mg of silica nanoparticles of were added to 50 mL of solution. After 24 h, the pH of the solution was read. As shown in Fig. 4, pH_{zpc} for silica nanoparticles is approximately 6.2.

3.2.2. pH effect

The results of pH effect on the adsorption capacity and removal efficiency of RY 42 dye were investigated by silica nanoparticles (Fig. 5). The pH studied in this research for the reactive dye yellow 42 is in the range 3–11. According to the diagram, with increasing pH, the removal efficiency and equilibrium adsorption capacity have decreased, so that at pH = 3, it has the highest removal efficiency of 66.1% and the equilibrium adsorption capacity is 6.61 mg/g. Also, the lowest removal efficiency at pH = 11 is 7.8% and the equilibrium adsorption capacity is 0.78 mg/g.

The pH of the solution is one of the main and influential factors in the adsorption studies because the change in pH changes the structure, the polluting agent groups and the electric charge of the adsorbent surface that is available to the contaminant, which ultimately leads to a reduction or increases the absorption process.

At acidic pH_s there are many hydrogen atoms, so it leads to higher adsorption to electrostatic attractions between negatively charged dye anions and a positively charged cell surface. Also, hydrogen ions bind to dye and adsorbent molecules, while in alkaline environments, the release of OH^- ions causes electrostatic repulsion. The OH^- ions are smaller in size than color molecules and easily adhere to the adsorbent surface, thus causing a dilution between the color molecules and the OH^- ion, which ultimately leads to electrostatic repulsion and reduced adsorption capacity.

In a study conducted by Yousaf [41], the results showed that the maximum equilibrium adsorption capacity at pH = 1 was equal to 30 mg/g. In another study performed by Jiang et al. [42], the results showed that at pH_s less than 3.3 it has the highest adsorption capacity, so that at pH = 1 the adsorption capacity is equal to 55 mg/g.

3.2.3. Effect of adsorbent dosage

Diagram shows the effect of the adsorbent dose on the adsorption capacity and reactivity of the RY 42

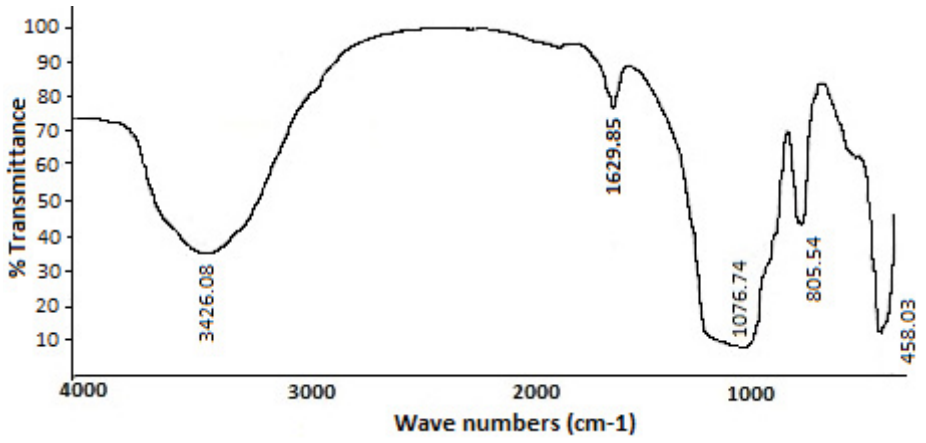

Fig. 1. FTIR spectrum of silica nanoparticles.

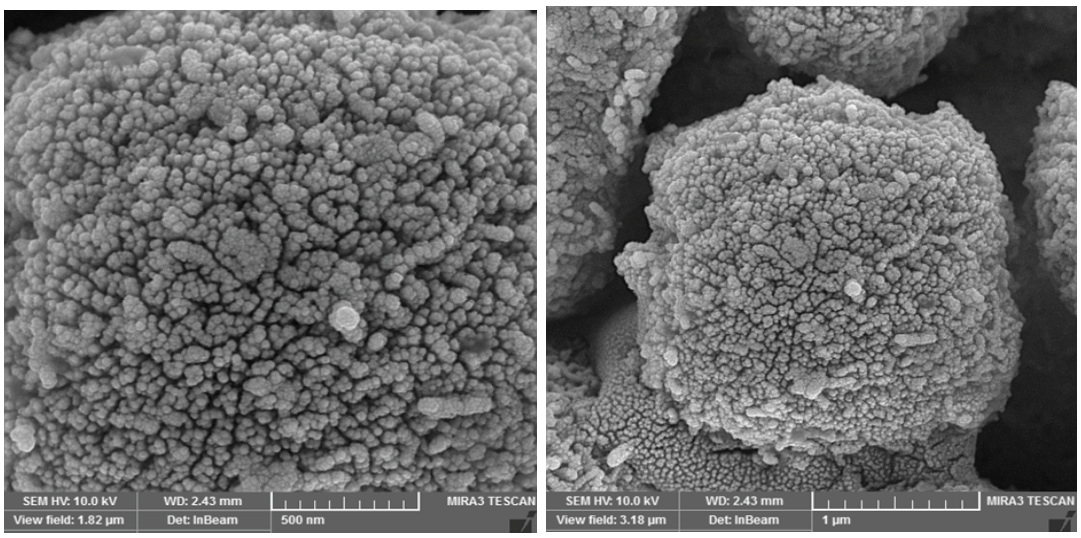

Fig. 2. Scanning electron microscopy images of silica nanoparticles.

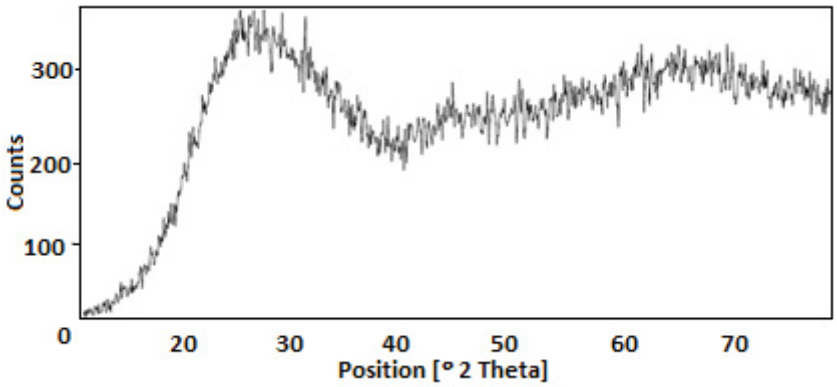

Fig. 3. XRD determination of silica nanoparticles.

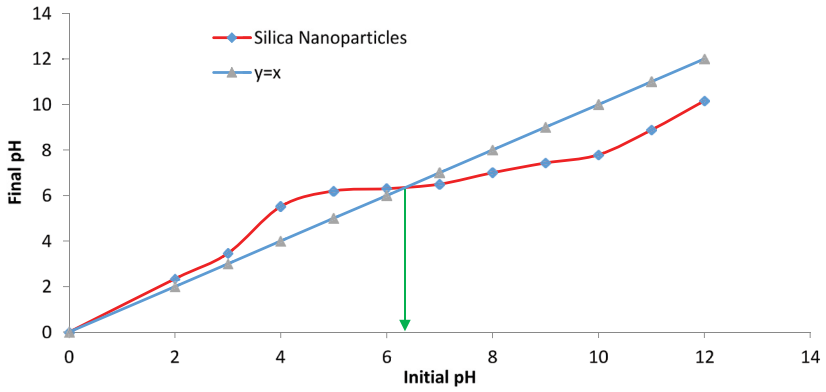

Fig. 4. Determination of pH_{zpc} for silica nanoparticles.

dye by silica nanoparticles. According to the diagram, the adsorption capacity of RY 42 dye decreased with increasing the adsorbent dose from 0.1 to 0.6 g/L and changed from 17.5 to 2.35 mg/L. Equilibrium absorption capacity was obtained in doses of 0.2, 0.3, 0.4 and 0.5 equal 6.6, 3.6, 3.9 and 1.4 mg/g, respectively.

According to Fig. 2, the adsorption capacity of RY 42 dye decreased with increasing the adsorbent dose from

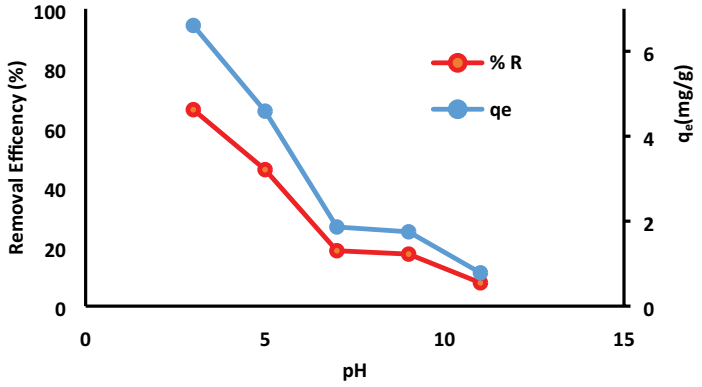

Fig. 5. Effect of initial pH on the efficiency and adsorption capacity of silica nanoparticles (Initial Reactive Yellow dye concentration 42 = 20 ppm, adsorbent dose = 0.2 g/L, contact time = 120 min).

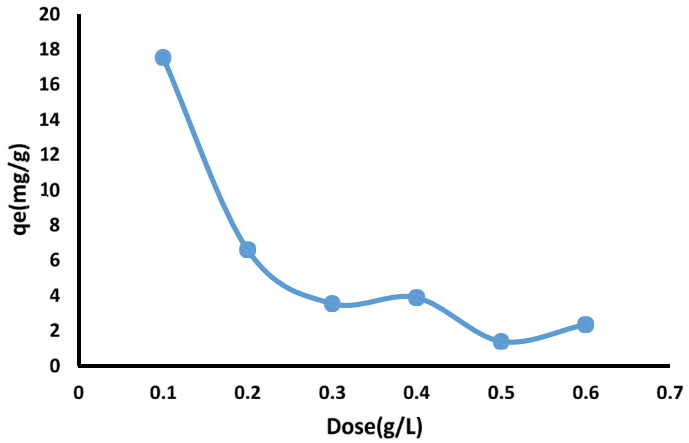

Fig. 6. Effect of adsorbent dose on the removal efficiency of RY 42 dye by silica nanoparticles (pH = 3, initial concentration of Reactive Yellow dye 42 = 20 ppm, time = 120 min).

0.1 to 0.6 g/L and changed from 17.5 to 2.35 mg/g. The reason is that with increasing the dose, the equilibrium adsorption capacity decreases. First, because the volume and concentration of the dye are constant, increasing the adsorbent mass saturates the adsorption sites through the adsorption process, and second, decreases the adsorption capacity due to particle accumulation which is the result of high adsorbent mass. Such aggregation leads to non-use of the total adsorbent surface. On the other hand, increasing the dose more than the optimal amount leads to a decrease in efficiency. A similar trend was observed in studies conducted by Kamranifar et al. [43].

It can also be stated that the reduction of the adsorption rate can be related to the anionic structure of RY 42 and the bar electricity of the adsorbent surface. In alkaline and acidic environments, the bar electricity of the adsorbent surface is negative and positive, respectively. In this case, the dye molecules are adsorbed in the acidic environment based on the electrostatic attraction of the surface. In a study by Özbay et al. [44], the results showed that the maximum adsorption capacity was obtained at the adsorbent dose of 0.05 mg/g and decreased with increasing dose.

3.2.4. Influence of initial concentration and contact time

The results of the effect of the RY 42 dye initial concentration on its adsorption capacity at different times by silica nanoparticles are shown in Fig. 7. As can be seen, the removal efficiency decreases with increasing initial concentration, and the removal efficiency increases with increasing contact time. RY 42 dye removal efficiency after 120 min for each of the concentrations of 10, 20, 30, 40 and 50 mg/L are equal to 94.1%, 87.7%, 56.1%, 27% and 10.74%. As a result, the highest removal percentage is related to the initial concentration of 10 mg/L and the contact time is 120 min.

At high dye concentrations, due to the saturation of the adsorption site, the removal efficiency is constant and uniform. Increasing the initial concentration can also be attributed to the drift that repels pollutant molecules and prevents dye adsorption on the adsorbent. In a study conducted by Zhu et al. [45], the results showed that the highest removal efficiency was obtained at the lowest concentration (10 mg/L).

Also, with increasing contact time, the removal efficiency increases. Contact time is one of the important

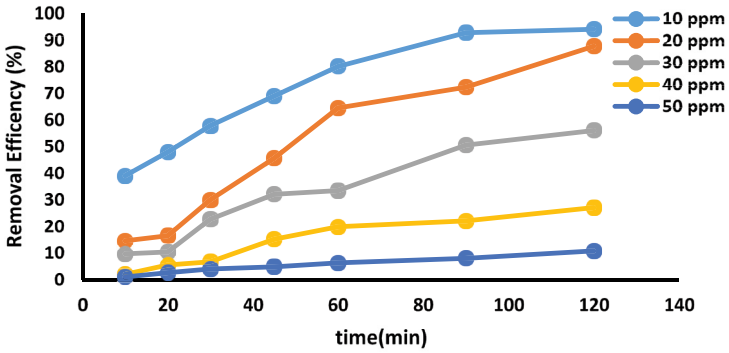

Fig. 7. Effect of initial solution concentration on the absorption rate of RY 42 dye at different times by silica nanoparticles (pH = 3, adsorbent dose = 0.1 g/L).

variables in the adsorption process, because with increasing contact time, the removal efficiency and also the adsorption capacity increase. In this study, the removal efficiency was faster during the early times and then slowed down. This may be due to the reduction of active points on the adsorbent surface and the decrease in the concentration of the RY 42 dye, because in the first minutes of adsorption, many empty sites are available. After a certain period of time, these places are occupied by dye molecules so that the removal efficiency increases with increasing the contact time and is fixed at a certain time, and then the amount of adsorption and desorption is in equilibrium. In a study conducted by Mahvi and Heibati [46], the results showed that the highest removal efficiency was at a concentration of 30 mg/L and a contact time of 120 min.

3.2.5. Investigation of RY 42 dye adsorption isotherms

The parameters of the Langmuir and Freundlich isotherm models for the RY 42 dye adsorption process by silica nanoparticles are shown in Table 1. According to linear regression calculations, the Brunauer–Emmett–Teller (BET) model is more suitable for adsorption data in the concentration range under the value of R^2 = 0.98 compared to other isothermal models for the adsorption of RY 42 dye by silica nanoparticles. The Langmuir isotherm with a correlation coefficient of R^2 = 0.94 is also a suitable isotherm for the adsorption of RY 42 dye by silica nanoparticles.

Balarak et al. [47] study shows the agreement of isothermal data with Langmuir model which is consistent with the result of the present study. One of the variables in the Langmuir isotherm is the R_L parameter, which is obtained from the following equation.

$$R_L = \frac{1}{1+\left(K_L \times C_0\right)} \tag{9}$$

where R_L value assumes the nature and the feasibility of adsorption process, K_L (L/mg) is the Langmuir constant related to the energy of adsorption and C_0 (mg/L) is the initial dye concentration.

Regarding to Eq. (8); If R_L = 1, the absorption is linear, if R_L = 0, the absorption is irreversible; if 1 < R_L < 0, the adsorption is desirable [47]. According to Table 1, the value is R_L = 0.02, which indicates the optimal adsorption of RY 42 dye on silica nanoparticles. Also, the q_{max} value of 19.47 mg/g silica nanoparticles was obtained, which shows the adherence of the adsorption process to the BET model, which evolved into the Langmuir model. This means that the adsorbent does not adsorb more than one molecule per location, in which case a layer of molecules will be adsorbed on the silica nanoparticles. In a study conducted by Salahshor et al. [48], the results showed that the adsorption process follows the Langmuir model with a rate of R^2 = 0.99.

Table 1
Isotherm models parameters for the RY 42 dye adsorption process by silica nanoparticles

Amounts	Coefficients	Isotherm type
Langmuir	q_{max} (mg/g)	19.47
	K_L (L/mg)	1.63
	R_L	0.02
	R^2	0.94
Freundlich constants	K_f	11.76
	$1/n$	0.18
	n_F	5.53
	R^2	0.65
BET constants	$1/A{\cdot}X_m$	0.0025
	$(A–1)/(A{\cdot}X_m)$	0.1104
	A	1
	X_m	9
	R^2	0.98
Temkin constants	A_T (L/mg)	210.46
	B_T (J/mol)	2.3
	R^2	0.63
Dubinin–Radushkevich constants	q_m (mg/g)	17.8
	E (kJ/mol)	2.19
	R^2	0.97

3.2.6. Investigation of adsorption kinetics in the process of RY 42 dye adsorption

In this study, the applicability of pseudo-first-order and pseudo-second-order kinetic models was investigated by

studying the adsorption kinetics at different initial concentrations of the adsorbent. The pseudo-first-order kinetics model is obtained by plotting logs in terms of log ($q_e - q_t$) against t and pseudo-second-order kinetics in terms of t/q_t vs. t. The pseudo-first-order kinetic graph is used to obtain the coefficient R^2 and the constant value K_1 as well as q_e, and the pseudo-second-order kinetic graph is used to obtain K_2, R^2 and q_e which is obtained by calculating the slope and width from the origin of the graph. Figs. 8 and 9 show the pseudo-first-order and pseudo-second-order kinetic models for the adsorption of the RY 42 dye by silica nanoparticles. In this study, the applicability of pseudo-first-order and pseudo-second-order kinetic models was investigated by studying the adsorption kinetics at different initial concentrations of the adsorbent. Comparison of R^2 coefficient values in the two studied kinetic models (Table 2) shows that the process of adsorption of RY 42 dye by silica nanoparticles follows the pseudo-second-order kinetic.

In this study, obtaining a coefficient of R^2 equal to 0.72 indicates the adaptation of the adsorption process from a quasi-quadratic kinetic model. The results of a study conducted by Malakootian and Macky [49] show that the adsorption rate of humic acid follows the pseudo-second-order kinetics with a correlation coefficient of 0.9936.

3.2.7. Investigation of temperature effect and thermodynamics of the yellow reactive dye 42 adsorption process

Another criterion that is important in the adsorption process is the determination of thermodynamic coefficients. Thermodynamic factors such as entropy changes, entropy changes and Gibbs free energy can be investigated using the equilibrium constant with temperature in equilibrium. By drawing a linear graph of Gibbs free energy changes with temperature, the slope of the entropy change line and also the width from the origin of the enthalpy changes, the absorption process is examined. The negative

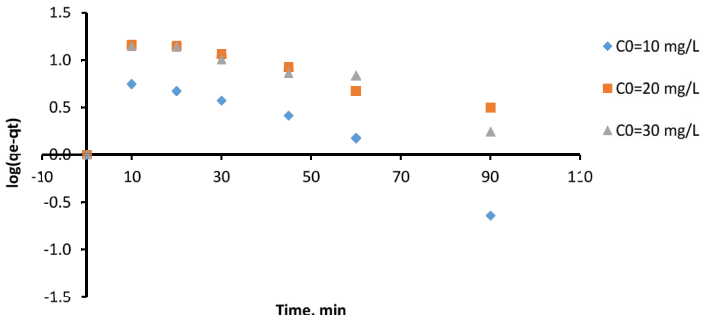

Fig. 8. Application of pseudo-first-order kinetic model for adsorption of RY 42 dye by silica nanoparticles.

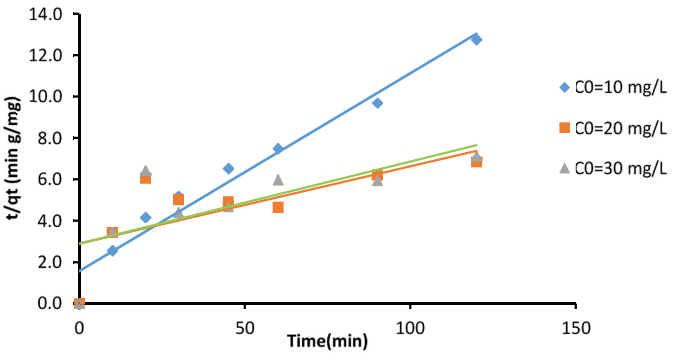

Fig. 9. Application of pseudo-second-order kinetic model for adsorption of RY 42 dye by silica nanoparticles.

Table 2
Coefficients of calculated kinetic models of RY 42 dye adsorption by silica nanoparticles

C_0 (mg/L)	Pseudo-first-order kinetic			Pseudo-second-order kinetic			$q_{e,exp}$ (mg/g)
	K_1 (min^{-1})	q_e (mg/g)	R^2	K_2 (g/mg min)	q_e (mg/g)	R^2	
10	0.03	5.3	0.7	0.01	10.46	0.99	9.51
20	0.03	12.53	0.4	0	26.78	0.94	17.64
30	0.03	12.34	0.44	0	25.28	0.72	16.92

sign of Gibbs free energy (ΔG) changes indicates that the adsorption process is spontaneous. Positive enthalpy (ΔH) changes indicate that the process is calorific. Entropy changes (ΔS) indicate an increase in irregularities in the interface between the adsorbent and the adsorbent.

Figs. 10 and 11 show the effect of temperature and thermodynamics in the adsorption process of RY 42 dye by silica nanoparticles. According to these figures and thermodynamic parameters of Table 3, it can be seen that with increasing temperature, the rate of adsorption and RY 42 dye removal efficiency increased, so that at the highest temperature (50°C) the highest capacity absorption (18.27 mg/g) can be observed. The thermodynamic parameters of RY 42 dye adsorption such as ΔG was negative, ΔS and ΔH were positive.

After calculating the constant thermodynamic equilibrium for different temperatures and calculating the corresponding free energy, the $\ln k_d$ diagram was plotted against $1/T$. If the absorption increases with increasing temperature, it is a sign that the reaction in removing the contaminant is endothermic. In this experiment, as can be seen, the Reactive Yellow dye removal efficiency increased with increasing ambient temperature. In a study conducted by Naghizadeh and Ghofouri [50] in a study, they concluded that the adsorption process is natural, spontaneous and endothermic.

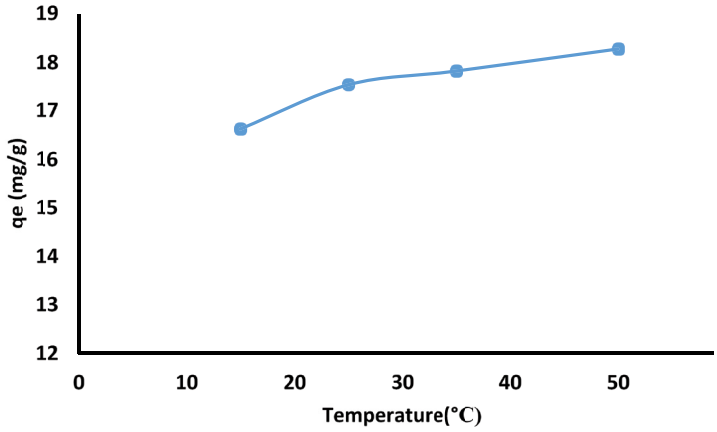

Fig. 10. Effect of temperature on the adsorption process of RY 42 dye by silica nanoparticles (pH = 3, adsorbent dose = 0.1 g/L, solution volume = 100 mL, initial dye concentration = 20 ppm).

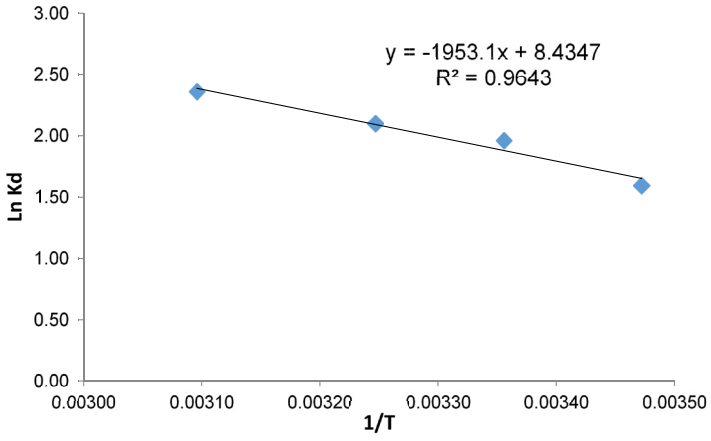

Fig. 11. Linear plot of $\ln k_d$ vs. $1/T$ for surface adsorption of RY 42 dye by silica nanoparticles.

Table 3
Thermodynamic parameters of RY 42 dye adsorption by silica nanoparticles

Adsorbent	ΔG (kJ/mol)				ΔH	ΔS
Temperature (Kelvin)	288	298	308	323	(kJ/mol)	(J/mol K)
Silica nanoparticles	–3.28	–4.68	–5	–5.38	16238.25	70.12

4. Conclusion

According to the results of this study, the maximum removal of RY 42 dye at pH was equal to 3 with 66.1% and the best optimal dose was 0.1 g/L. As the pollutant concentration increased, the removal percentage and consequently the efficiency decreased, and the isotherm and kinetics followed the Langmuir and the quasi-quadratic model. Also, the highest percentage of RY 42 dye removal was at pH = 3, initial concentration = 10 ppm, adsorbent dose = 0.1 g/L and contact time = 120 min equal to 94.1%. Gibbs free energy changes (ΔG), enthalpy changes (ΔH) and entropy changes (ΔS) were obtained in this study. Since (ΔG) is negative, (ΔH) is positive and (ΔS) is positive, the process is endothermic and spontaneous. According to the results, the adsorption process by silica nanoparticles is a suitable adsorption option for the removal of RY 42 dye from aqueous solutions and wastewater, and can be used as an efficient and suitable adsorbent.

Acknowledgment

The authors of the article express their gratitude to the Deputy of Research and Technology of Birjand University of Medical Sciences for financially supported this project. The article is the result of the research project approved by the Vice Chancellor for Research and Technology of Birjand University of Medical Sciences.

References

[1] E. Bazrafshan, F. Kord Mostafapour, Evaluation of color removal of Methylene blue from aqueous solutions using plant stem ash of Persica, J. North Khorasan Univ. Med. Sci., 4 (2012) 523–532.
[2] M. Shirzad-Siboni, S. Fallah, S. Tajasosi, Removal of Acid Red 18 and Reactive Black 5 dyes from aquatic solution by using of adsorption on *Azollafiliculoides*: a kinetic study, J. Guilan Univ. Med. Sci., 3 (2014) 42–50.
[3] S. Sobhanardakani, Evaluation of carbon nanotubes efficiency for removal of Janus Green dye from ganjnameh river water sample, J. Health Dev., 3 (2015) 282–292.
[4] N. Yousefi, A. Fatehizadeh, A. Ahmadi, A. Rajabizadh, A. Toolabi, M. Ahmadian, The efficiency of modified wheat brad in Reactive black 5 dye removal from aqueous solutions, J. Health Dev., 3 (2013) 157–169.
[5] J. Ghobadi, M. Arami, H. Bahrami, Modification of multi-walled carbon nanotubes and its application for removal of Direct Blue 86, J. Color Sci. Technol., 3 (2013) 103–112.
[6] R. Bhattacharyya, S.K. Ray, Removal of Congo red and methyl violet from water using nano clay filled composite hydrogels of polyacrylic acid and polyethylene glycol, Chem. Eng. J., 260 (2015) 269–283.
[7] Z. Noorimotlagh, M. Javaheri, Z. Rahmati, H. Nourmoradi, Evaluating the performance of Limecoagulant using synthetic polymer in dye removal from textile wastewater, J. Ilam Univ. Med. Sci., 22 (2014) 14–23.
[8] H. Alidadi, H. Karimian, E. Bazrafshan, A.A. Najaf Poor, S. Rafe, A Survay on dye removal from colored textile wastewater using multi-walled carbon nanotubes and palm ash as a natural adsorbent, J. Res. Environ. Health, 1 (2015) 10–19.
[9] A. Naghizadeh, A.H. Mahvi, A.R. Mesdaghinia, Application of MBR technology in municipal wastewater treatment, Arabian J. Sci. Eng., 36 (2011) 3–10.
[10] M. Ghaneian, M. Dehvari, N. Jourabi Yazdi, M. Mootab, B. Jamshidi, Evaluation of efficiency of Russian knapweed flower powder in removal of Reactive blue 19 from synthetic textile wastewater, J. Rafsanjan Univ. Med. Sci., 12 (2013) 831–842.
[11] M. Shirmardi, F. Khodarahmi, M. Heidari Farsani, A. Naeimabadi, M. Vosughi Niri, Application of oxidized multiwall carbon nanotubes as a novel adsorbent for removal of Acid red 18 dye from aqueous solution, J. North Khorasan Univ. Med. Sci., 4 (2012) 335–346.
[12] H. Nourmoradi, S. Zabihollahi, H. Pourzamani, Removal of a common textile dye, navy blue (NB), from aqueous solutions by combined process of coagulation–flocculation followed by adsorption, Desal. Water Treat., 57 (2016) 1–12.
[13] A. Vanamudan, P. Pamidimukkala, Chitosan, nanoclay and chitosan–nanoclay composite as adsorbents for Rhodamine-6G and the resulting optical properties, Int. J. Biol. Macromol., 14 (2015) 127–135.
[14] K. Naddafi, M. Gholami, Removal of Reactive Red 120 from aqueous solutions using surface modified natural zeolite, Iran J. Health Environ., 7 (2015) 277–288.
[15] A.R. Rahmani, G. Asgari, M. Farrokhi, Removal of Reactive Black 5 (RB5) dye from aqueous solution using adsorption onto strongly basic anion exchange resin: equilibrium and kinetic study, Iran J. Health Environ., 5 (2013) 509–518.
[16] H. Jafari Mansoorian, A.H. Mahvi, Feasibility of extracted activated carbon from the leaves of mesquite (Prosopis) as new adsorbents in the removal of Reactive dyes Red 198 and Blue 19, J. Health Dev., 3 (2014) 114–127.
[17] M. Gholami, H. Mohammadi, S. Mirhosseini, A. Ameri, Z. Javadi, Evaluation of powdered-activated carbon treatment (PACT) process in textile dye removal, ZUMS J., 61 (2007) 59–70.
[18] A. Naghizadeh, M. Kamranifar, A.R. Yari, M.J. Mohammadi, Equilibrium and kinetics study of reactive dyes removal from aqueous solutions by bentonite nanoparticles, Desal. Water Treat., 97 (2017) 329–337.
[19] M.R. Rezaee-Mofrad, M.B. Miranzadeh, M. Pourgholi, H. Akbari, R. Dehghani, Evaluating the efficiency of advanced oxidation methods on dye removal from textile wastewater, Feyz J. Kashan Univ. Med. Sci., 17 (2013) 9–32.
[20] E. Derakhshani, A. Naghizadeh, Ultrasound regeneration of multi wall carbon nanotubes saturated by humic acid, Desal. Water Treat., 52 (2014) 7468–7472.
[21] Z. Eren, F.N. Acar, Adsorption of Reactive Black 5 from an aqueous solution: equilibrium and kinetic studies, Desalination, 194 (2006) 1–10.
[22] V. Gupta, Application of low-cost adsorbents for dye removal–a review, J. Environ. Manage., 90 (2009) 2313–2342.
[23] H. Jafari Mansoorian, A.H. Mahvi, F. Kord Mostafapoor, M. Alizadeh, Equilibrium and synthetic studies of methylene blue dye removal using ash of walnut shell, J. Health Field., 3 (2013) 48–55.
[24] S. Ling, C. Yee, H. Eng, Removal of a cationic dye using deacetylated chitin (chitosan), Res. J. Appl. Sci., 3 (2011) 1445–1448.
[25] L. Pietrelli, I. Francolini, A. Piozzi, Dyes adsorption from aqueous solutions by chitosan, Sep. Sci. Technol., 50 (2015) 1101–1107.
[26] S. Moussavi, M. Emamjomeh, M. Ehrampoush, M. Dehvari, S. Jamshidi, Removal of Acid Orange 7 dye from synthetic textile wastewater by single-walled carbon nanotubes: adsorption studies, isotherms and kinetics, J. Rafsanjan Univ. Med. Sci., 12 (2014) 907–918.
[27] A. Naghizadeh, A. Karimi, E. Derakhshani, A. Esform, Single-walled carbon nanotubes (SWCNTs) as an efficient adsorbent for removal of reactive dyes from water solution: equilibrium, kinetic, and thermodynamic, Environ. Qual. Manage., (2021), doi: 10.1002/tqem.21753 (in Press).
[28] M. Samarghandi, M. Noori Sepehr, M. Zarrabi, M. Norouzi, F. Amraie, Mechanism and removal efficiency of CI Acid Blake 1 by pumice stone adsorbent, Iran J. Health Environ., 3 (2011) 399–410.
[29] G. Ghanizadeh, G. Asgari, Removal of Methylene Blue dye from synthetic wastewater with bone char, Iran J. Health Environ., 2 (2009) 104–113.
[30] M. Ghaneian, T. Jasemizad, F. Sahlabadi, M. Miri, M. Mootab, Survey the efficiency of barberry stem powder in removal of the

Reactive Blue 19 from textile industrial wastewater, J. Rafsanjan Univ. Med. Sci., 13 (2014) 631–640.
[31] A. Mahvi, B. Heibati, Removal efficiency of azo dyes from textile effluent using activated carbon made from walnut wood and determination of isotherms of Acid Red 18, J. Health Hyg., 3 (2011) 7–15.
[32] A. Naghizadeh, S. Nasseri, A.H. Mahvi, R.R. Kalantary, A. Rashidi, Continuous adsorption of natural organic matters in a column packed with carbon nanotubes, J. Environ. Health Sci. Eng., 11 (2013) 14, doi: 10.1186/2052-336X-11-14.
[33] M. Samadi, M. Saghi, K. Ghadiri, M. Hadi, M. Beikmohammadi, Performance of simple Nano Zeolite Y and modified Nano Zeolite Y in phosphor removal from aqueous solutions, Iran J. Health Environ., 3 (2010) 27–36.
[34] M. Chauhan, B. Sharma, R. Kumar, G.R. Chaudhary, A.A. Hassan, S. Kumar, Green synthesis of CuO nanomaterials and their proficient use for organic waste removal and antimicrobial application, Environ. Res., 168 (2019) 85–95.
[35] M.N. Nadagouda, G. Hoag, J. Collins, R.S. Varma, Green synthesis of Au nanostructures at room temperature using biodegradable plant surfactants, Cryst. Growth Des., 9 (2009) 4979–4983.
[36] S.J. Ikhmayies, Characterization of nanomaterials. JOM, 66 (2014) 28–29.
[37] J. Lu, Y. Li, X. Yan, B. Shi, D. Wang, H. Tang, Sorption of atrazine onto humic acids (HAs) coated nanoparticles, Colloids Surf., A, 347 (2009) 90–96.
[38] Z. Warrior, L. Shahbazi, A. Badiee, Synthesis and modification of nano-cavity silica surface with mono and dendrimer amine groups in order to remove methylene blue color from effluent, Water Wastewater J., 27 (2016) 19–28.
[39] A. Naghizadeh, H. Shahabi, E. Derakhshani, F. Ghasemi, Synthesis of nanochitosan for the removal of fluoride from aqueous solutions: a study of isotherms, kinetics, and thermodynamics, Fluoride, 50 (2017) 256–268.
[40] A. Naghizadeh, S.J. Mousavi, E. Derakhshani, M. Kamranifar, S.M. Sharifi, Fabrication of polypyrrole composite on perlite zeolite surface and its application for removal of copper from wood and paper factories wastewater, Korean J. Chem. Eng., 35 (2018) 662–670.
[41] M. Yousaf, Removal of RY 42 anionic dye pollutant from aqueous solution using novel reusable adsorbent prepared from water chestnut peel and fruit, Int. J. Curr. Eng., 8 (2018) 33–40.
[42] Z. Jiang, J. Xie, D. Jiang, Z. Yan, J. Jing, D. Liu, Enhanced adsorption of hydroxyl contained/anionic dyes on non-functionalized Ni@SiO_2 core–shell nanoparticles: kinetic and thermodynamic profile, Appl. Surf. Sci., 292 (2014) 301–310.
[43] M. Kamranifar, F. Masoudi, A. Naghizadeh, M. Asri, Fabrication and characterization of magnetic cobalt ferrite nanoparticles for efficient removal of humic acid from aqueous solutions, Desal. Water Treat., 144 (2019) 233–242.
[44] N. Özbay, A. Yargıç, R.Z. Yarbay-Şahin, E. Önal, Full factorial experimental design analysis of reactive dye removal by carbon adsorption, J. Chem., 2013 (2013) 234904, doi: 10.1155/2013/234904.
[45] H.Y. Zhu, R. Jiang, Y.Q. Fu, J.H. Jiang, L. Xiao, G.M. Zeng, Preparation, characterization and dye adsorption properties of γ-Fe_2O_3/SiO_2/chitosan composite, Appl. Surf. Sci., 258 (2011) 1337–1344.
[46] A.H. Mahvi, B. Heibati, Removal efficiency of azo dyes from textile effluent using activated carbon made from walnut wood and determination of isotherms of Acid Red 18, J. Health Ardabil Univ. Med. Sci., 3 (2010) 7–15.
[47] D. Balarak, H. Abasizdeh, Z. Jalalzayi, P. Rajiv, P. Vanathi, Batch adsorption of Acid Blue 113 dye from aqueous solution using surfactant-modified zeolite, Indian J. Environ. Prot., 40 (2020) 927–933.
[48] Z. Salahshor, A. Shahbazi, A. Badiee, Synthesis and modification of nano-cavity silica surface with mono and dendrimer amine groups in order to remove methylene blue color from effluent, J. Water Wastewater, 27 (2016) 19–28.
[49] M. Malakootian, M. Macky, Assessing the performance of removal Acid Orange 7 bye from aqueous solutions and textile waste water by nanoporous MCM-41 silica absorbent functionalized by diamine group, J. Rafsanjan Univ. Med. Sci., 15 (2016) 37–50.
[50] A. Naghizadeh, M. Ghofouri, Synthesis of low cost nanochitosan from Persian Gulf shrimp shell for efficient removal of Reactive Blue 29 (RB29) dye from aqueous solution, Iran. J. Chem. Chem. Eng., 38 (2019) 93–103.